A lateral flow immunoassay with self-sufficient microfluidic system for enhanced detection of thyroid-stimulating hormone 🄴🄿

🄳 Santosh Kumar Bikkarolla, Sara E. McNamee, Stuart McGregor, Paul Vance, Helen McGhee, Emma L. Marlow, and 🄳 James McLaughlin

COLLECTIONS

Paper published as part of the special topic on Chemical Physics, Energy, Fluids and Plasmas, Materials Science and Mathematical Physics

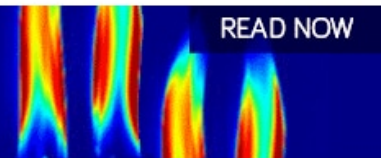🄴🄿   This paper was selected as an Editor's Pick

View Online   Export Citation   CrossMark

A lateral flow immunoassay with self-sufficient microfluidic system for enhanced detection of thyroid-stimulating hormone ᴇᴘ

View Online   Export Citation   CrossMark

Santosh Kumar Bikkarolla,[1,a] (iD) Sara E. McNamee,[1] Stuart McGregor,[2] Paul Vance,[2] Helen McGhee,[2] Emma L. Marlow,[1] and James McLaughlin[1,a] (iD)

AFFILIATIONS

[1] School of Engineering, Engineering Research Institute, University of Ulster, Newtownabbey BT37 0QB, United Kingdom
[2] Randox Laboratories Ltd., 55 Diamond Road, Crumlin, County Antrim BT29 4QY, United Kingdom

[a] Authors to whom correspondence should be addressed: s.k.bikkarolla@ulster.ac.uk and jad.mclaughlin@ulster.ac.uk

ABSTRACT

We report a self-sufficient microfluidic paper-based lateral flow immunoassay device (μLFD) for highly sensitive detection of the thyroid-stimulating hormone (TSH). Fabrication of the paper microchannels involves engraving the nitrocellulose membrane with a CO_2 laser to create narrow flow paths, which constrain the fluid flow over the test zone. The proposed microchannel modified devices were studied for detection of the TSH using gold nanoparticles as labels. The effect of such microchannel modified LFDs has led to an improvement in sensitivity by nine times and the limit of detection by 6.6 times due to the slow flow rate of the sample compared with the traditional LFD. In addition, the binding of gold nanoparticles over the test line is more uniform in the case of the μLFD, thus minimizing leading-edge effects, resulting in more accurate quantitative analysis. The proposed strategy offers great potential for multiplex detection of biomarkers with increased sensitivity without introducing any hydrophobic materials to the LFD.

I. INTRODUCTION

Lateral flow immunoassay devices (LFDs) are suitable for rapid detection of analytes from a finger prick blood sample in low resource settings, are inexpensive and self-powered, and require a small volume of the blood sample. The World Health Organization (WHO) recognizes the importance of point of care (POC) devices such as LFDs in diagnosing diseases and has established criteria for evaluating such devices. Given the acronym "ASSURED," the criteria specify that devices should be "affordable, sensitive, specific, user-friendly, rapid and robust, equipment-free, and deliverable to end users." Current LFDs are simple wicking-based devices, which use gold nanoparticles (AuNPs) for detection of biomarkers. However, extensive use of LFDs is limited due to the lack of sensitivity and reproducibility and due to quantitative analysis issues. One of the main reasons for the lack of sensitivity is that the most commonly observable labels such as AuNPs are not particularly sensitive. Labels such as carbon nanomaterials,[1–5] latex beads,[1] fluorescent europium

nanoparticles,[6] chemiluminescent labels,[7] horseradish peroxidase-conjugated AuNPs,[8] graphene oxide coated with AuNPs,[9] silver nanoparticles,[10] and platinum nanoparticles[11–13] have all been used to improve the performance of LFDs. There are several self-sufficient paper-based devices that have been reported, which improve the performance of the lateral flow assay in terms of reducing non-specific binding, improving quality of test lines, and limit of detection.[14–16] Zhang et al. have developed a self-contained microfluidic lateral flow assay device, which enables delivery of the reagent and the sample through capillary action from two separate flow paths to reduce non-specific binding of conjugate particles to the nitrocellulose (NC) membrane. In addition, to avoid the uneven flow due to the 2D microfluidic network, a liquid impermeable membrane was introduced to mix the reagent and sample flows uniformly across the test strip, which resulted in even test lines with good quantification capability.[17] Wang et al. have developed a self-powered microfluidic device that incorporates filter paper for separation of plasma from whole blood and an absorbent pad to induce capillary flow in the

channels for rapid multiplexed detection of biomarkers from whole blood.[18]

One of the critical factors that determine the performance of the assay is the immunoreaction time between the antigen and the capture antibody; thus, slower migration time of the sample over the test line leads to increased sensitivity. Recent reports have shown that decreasing the sample flow rate or stopping the flow temporarily on the membrane by using novel techniques such as wax printing, PDMS deposition, and use of tunable delay shunts on NC membrane has led to improvement in LFD performance.[19–24] Rivas *et al.* have fabricated small diameter wax barriers at the starting of the NC membrane to slow the sample flow, which resulted in improvement in the limit of detection (LOD) by 2.6-fold when compared with the unmodified NC membrane.[19] Katis *et al.* constrained fluid flow in a 1 mm wide channel and improved sensitivity by 62 times and the LOD by 30 times when compared with an unmodified LFD.[23] Simple modifications to the shapes of the NC membrane, conjugate pad, and sample pad have also shown improvement in LFD performance.[25] Zadehkafi *et al.* have shown that LFDs with a trapezoidal shaped NC membrane having a narrow width at the absorbent pad and the position of the test line far from the conjugation pad have shown improved performance by decreasing the LOD from 10 mIU/ml to 5 mIU/ml and increased test line intensities by two times for the human chorionic gonadotropin biomarker when compared with normal LFDs.[26]

In this study, a self-sufficient microfluidic paper-based lateral flow immunoassay device (μLFD) was developed for sensitive detection of the thyroid-stimulating hormone (TSH). The fabricated narrow flow paths can constrain the same amount of fluid flow over the smaller test zone, resulting in enhanced detection and removal of the leading-edge binding effect. The narrow flow paths also act as self-contained resistors, which decrease the fluid flow rate and increase the immuno reaction time at the test line. Therefore, the narrow flow paths act as a self-sufficient microfluidic system for enhanced detection of the TSH. The fabrication process involves engraving with a CO_2 laser to burn the NC membrane across its thickness, according to the predesigned pattern.[27–30] The process of forming narrow flow paths is rapid: a typical NC membrane 2.5 cm wide and 35 cm long can be engraved within 24 min to produce 55 devices. The process does not require any additional hydrophobic materials, such as wax or photo-polymers, which can result either in adsorption of proteins or contamination of capture antibodies and decreases LFD performance.[27] The process of fabricating paper microchannels is highly reproducible and suitable for the bulk manufacturing process, enabling patterning techniques to be implemented in LFD applications.

To show the advantages of such paper microchannels, we have implemented the TSH as a model assay for a proof of principle study to demonstrate the feasibility of the modified μLFDs. The TSH is essential in maintaining the body's metabolism and energetics. The TSH plays a key role in developing physical and mental growth.[31] It is critical for the nervous, skeletal, and cardiovascular systems as well as in regulating body temperature, heartbeat, and cholesterol.[32–34] If a thyroid-related disease is untreated, several symptoms such as excessive gain or loss of weight, cold intolerance, increased heartbeat, infertility, and developing low bone density and a range of autoimmune diseases can be observed.[35,36] TSH levels are normally measured either with finger prick blood samples or blood obtained from the vein. The normal TSH concentration for healthy individuals is in the range of 0.5 μIU/ml–5 μIU/ml.[36,37] In the case of sub-clinical hypothyroidism, TSH levels are in the range of 5 μIU/ml–10 μIU/ml,[38] and TSH levels above 10 μIU/ml are considered thyroid failure.[39] Here, we demonstrate the potential applicability of μLFDs for the detection of TSH levels with nine times increased sensitivity and 6.6 times improved LOD when compared with traditional LFDs. The LOD by using μLFDs is 7.5 μIU/ml, making the new devices useful for detection of the TSH in the clinical range. In addition, the μLFD demonstrates potential feasibility for multiplex detection of various biomarkers.[40,41]

II. MATERIALS AND METHODS

A. Reagents and materials

The monoclonal mouse anti-TSH antibody (10-2428, Fitzgerald) and monoclonal mouse anti-TSH antibody (10-2426, Fitzgerald) were used as capture and detection anti-bodies, respectively. The TSH antigen derived from the human pituitary gland was obtained from the NIBSC. TSH calibrators in serum were obtained from Randox Laboratories. The nitrocellulose membrane (CN95, UniSart) was obtained from Sartorius. The absorbent pad (Ahlstrom Munksjö, A238, A222) was purchased from Kenosha Tapes. The backing card (width 80 mm and thickness 0.015 in.) was purchased from DCN. Carboxyl gold nanoparticles (40 nm, 40 OD) were obtained from Expedeon. N-(3-Dimethylaminopropyl)-N'-ethylcarbodiimide hydrochloride (EDC), phosphate buffered saline (PBS), 2-(N-morpholino) ethanesulfonic acid (MES), Tris-buffered saline (TBS), sodium phosphate monobasic monohydrate, sodium phosphate dibasic monohydrate, and sucrose were all purchased from Sigma-Aldrich.

B. Modification of gold nanoparticles (AuNPs) with antibodies

The TSH detection antibody was purified using an Amicon filter unit to remove any amine terminated molecules, which can interfere in the conjugation process, and the purified antibodies were resuspended in 10 mM potassium phosphate buffer of 7.4 pH. A AuNP-TSH antibody conjugate was prepared by following the recommended protocol from Expedeon.[42] In brief, AuNPs functionalized with the carboxyl group were used to covalently bind TSH antibodies by using water-soluble EDC.[43] To 50 μl of AuNP suspension (40 OD), 20 μl of 100 μg/ml TSH detection antibodies was mixed followed by addition of 20 μl of 1 mM EDC. The resultant solution was incubated for 30 min at room temperature. Then, 1 ml of TBS (containing 0.05% Tween) was added to the mixture and centrifuged at 6200 rpm at 10 °C for 10 min. The supernatant was carefully removed, and the pellet of the AuNP-antibody was resuspended in 90 μl of 1XTBS, 0.5% BSA, and 0.05% Tween to obtain 20 OD of the conjugate.

C. Fabrication of LFDs and μLFDs

LFDs were prepared in three different configurations—(1) traditional LFDs of 5 mm width, (2) single-channel μLFDs, and (3) multi-channel μLFDs consisting of three parallel channels—as shown in Fig. 1(b). Fabrication of μLFDs consists of two important steps, as shown in Fig. 1(a): (1) dispensing capture antibodies
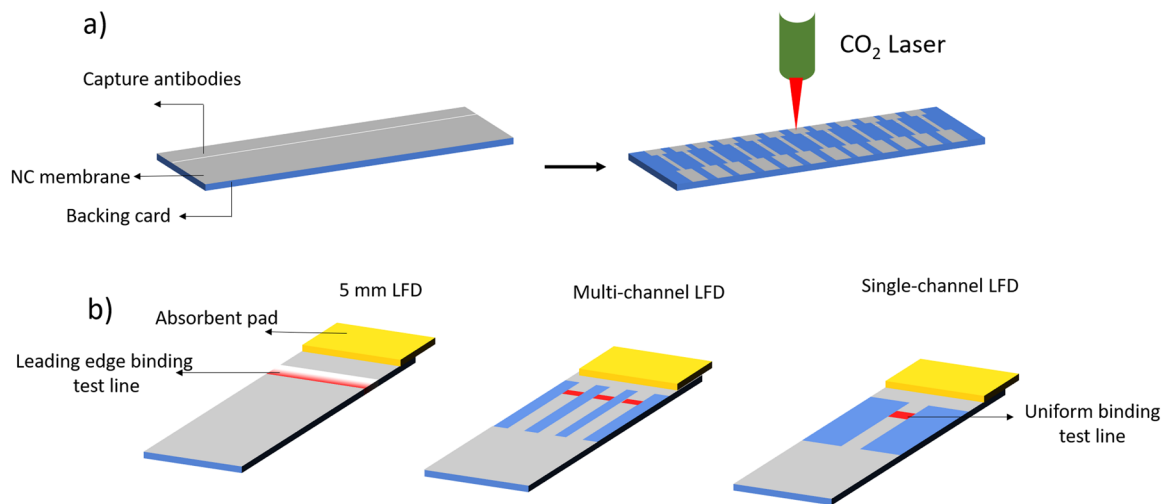
FIG. 1. (a) Fabrication process of μLFDs and (b) three different formats of LFDs: traditional LFDs of 5 mm width, multi-channel μLFDs consisting of three parallel channels, and single channel μLFDs.

on the NC membrane and (2) laser irradiation on the NC membrane. In step 1, the capture antibodies were diluted in 10 mM phosphate buffer containing 1% of sucrose to obtain a concentration of 1 mg/ml. The anti-TSH antibody (10-2428) was dispensed onto the NC membrane using a BioDot (ZX1010) dispensing platform at a flow rate of 1 μl/cm to obtain a test line width of 1 mm. Then, the NC membrane was dried in an oven at 37 $^\circ$C for 30 min. Step 2 was performed by a Universal Laser Systems VLS2.30 equipped with a 10.6 μm wavelength pulsed CO_2 laser system (25 W). A laser duty cycle of 7.5%, scan rate of 20 cm/s, and image density of 1000 ppi were used to fabricate paper microfluidic channels. After the fabrication process, the NC membrane was laminated onto a plastic backing card followed by the absorbent pad with 3 mm overlap on the NC membrane. We simplified the design of the LFD by eliminating the sample pad and the conjugate pad. Finally, strips were cut 5 mm wide and stored in aluminum foil bags with a desiccant to absorb moisture.

D. The lateral flow assay procedure

TSH antigen solutions of different concentrations ranging from 1000 μIU/ml to 5 μIU/ml were prepared in 10 mM PBS, a pH 8.0 buffer. To prepare the reaction solution, 5 μl of the Au conjugate (5 OD) was mixed with 45 μl of the reaction buffer (10 mM PBS, 1% BSA, and 0.05% Tween) and 10 μl of TSH antigen solution. Next, 60 μl of the reaction solution is added to each well of a 96-well plate. The LFD was immersed into the sample well and allowed to react until all the solution in the well diffused to the absorbent pad. After the formation of the test line, the LFDs were dried and scanned using an HP8600 scanner with 1200 dpi resolution, and the intensity of the test lines was deduced using ImageJ software. LOD is defined as the minimum concentration that is required to obtain a mean intensity three times higher than the standard deviation of the blank, without the antigen, when compared with the mean intensity of the

blank.[44,45] Each set of experiments was repeated three times in order to check the reproducibility of results.

III. RESULTS AND DISCUSSION

A number of antibodies for the TSH were sourced from different suppliers for suitability in LFDs. Different configurations (n = 19) with regard to the capture and detection antibodies were evaluated during the initial antibody screening and characterization process. Initial experiments focused on spotting antibodies on the NC membrane and assessing for sensitivity and non-specific binding. From this initial evaluation, it can be concluded that antibodies obtained from Fitzgerald looked the most promising and were used for the remainder of the study.

To evaluate the stability of the AuNP- TSH conjugate, UV-VIS spectra were collected before and after the conjugation process to measure the optical density (OD) of the conjugate. Figure 2 shows a successful conjugation on gold nanoparticles where the resonance peak is shifted to the right by about 4 nm (red shifted) due to the effect of conjugated protein on the plasmon resonance peak of the gold nanoparticle. In addition, the FWHM and OD of the conjugate are the same as those of the gold nanoparticles, indicating that the conjugate consists of monodispersed gold nanoparticles attached to the detector antibody.

To enhance the analytical sensitivity of LFDs for TSH detection, a new μLFD was developed to decrease the fluid flow rate without adding any additional components and maintaining the traditional format. Fabrication of paper microchannels using CO_2 was performed on the capture antibody deposited NC membrane, as shown in Fig. 1(a), to obtain uniform width of the test line. It was observed that dispensing antibodies using the BioDot on a patterned NC membrane resulted in an uneven test line shape due to the presence of the narrow flowpaths; therefore, antibodies were dispensed first. Due to the small spot size (70 μm) and the pulsed mode
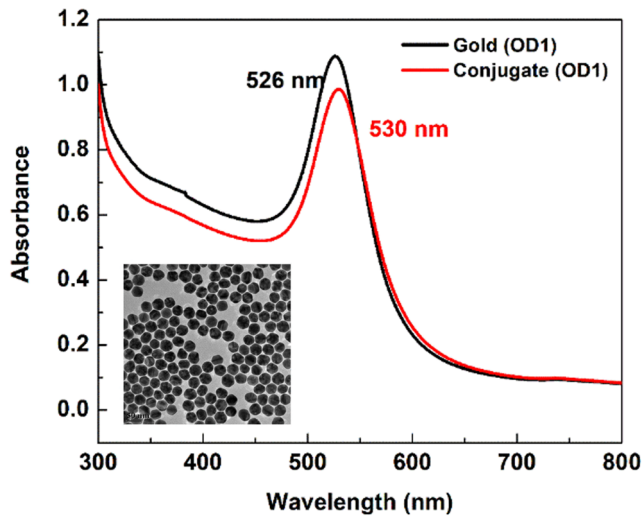
FIG. 2. Shows the UV-VIS spectra of 40 nm gold nanoparticles before and after conjugation (the inset shows the TEM image of the 40 nm gold nanoparticles).

operation of the CO_2 laser, antibodies did not burn during the engraving process of the NC membrane. By following this procedure, paper microchannels of 0.5 mm width were fabricated without damaging the antibodies. To fabricate the paper microchannels, the NC membrane next to the channels was completely etched to make the fluid flow constrained to the designed pathways, as shown in Fig. 1(b).

LFDs were prepared in three different configurations: (1) traditional LFDs of 5 mm width, (2) single-channel μLFDs, and (3) multichannel μLFDs consisting of three parallel channels, as shown in Fig. 1(b). Single-channel and multi-channel devices were fabricated with channel widths of 0.5 mm and 1 mm, respectively. The TSH

assay was evaluated on all the strips with varying concentrations, as shown in Fig. 3, and the intensities of the test line were evaluated using ImageJ. The color test lines were selected, and the average intensity values were measured. These values were subtracted from the background noise, which was measured by taking the average of the intensity values before and after the test lines for each individual strip.

First, the performance of the LFDs consisting of absorbent pads A222 and A238 was studied for the TSH assay. Absorbent pads A222 and A238 have wicking rates of 20 s/4 cm and 150 s/4 cm, respectively. The LFD laminated with A222 is referred to as the traditional LFD. The LFD laminated with A222 showed an LOD of 50 μIU/ml, while using an LFD laminated with A238, an LOD of 20 μIU/ml was obtained. This shows that using a lower wicking rate absorbent pad results in a 2.5-fold improvement in the LOD and an increase in test line intensities. In addition, leading-edge binding is observed more prominently on the LFD laminated with the A222 absorbent pad due to the high wicking rate.

To further improve the performance of the LFD, the NC membrane was patterned in the form of microchannels. For μLFDs, the absorbent pad A238 was used. For an analyte concentration of 1000 μIU/ml, the test line intensity increased 3.5 times on 0.5 mm width constriction when compared with traditional LFDs. It was observed that for lower concentrations, from 250 μIU/ml to 50 μIU/ml, the test line intensities were nine times higher on the 0.5 mm channel constriction when compared with traditional LFDs. For this device, the LOD was found to be 7.5 μIU/ml, a 6.6-fold enhancement when compared with the traditional LFD.

In the case of multiplex μLFDs of 0.5 mm channel width, the test line intensities are three times higher than those of traditional LFDs at an antigen concentration of 1000 μIU/ml. For analyte concentrations from 250 μIU/ml to 50 μIU/ml, the test line intensities were six times higher when compared with traditional LFDs. Multiplex μLFDs with 0.5 mm channel width exhibited 7.5 μIU/ml as the LOD, which indicates a 6.6-fold increase in the LOD when compared
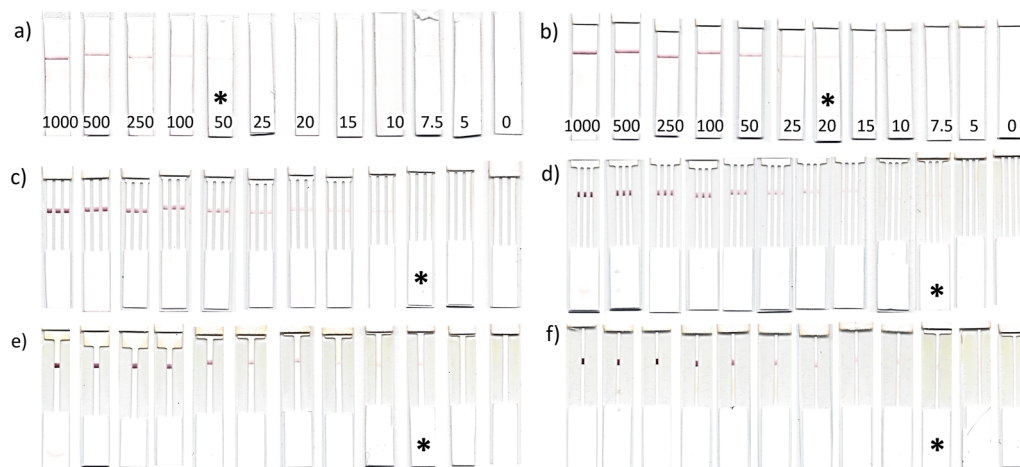

FIG. 3. Scanned images of LFDs and μLFDs after the TSH assay performed at various concentrations ranging from 1000 μIU/ml to 5 μIU/ml: (a) the LFD of 5 mm width attached to the A222 absorbent pad (considered as the traditional LFD), (b) the LFD of 5 mm width attached to the absorbent A238, (c) and (d) multiplex channel μLFDs of 1 mm and 0.5 mm channel widths, and (e) and (f) single channel μLFDs of 1 mm and 0.5 mm channel widths. The asterisks (∗) indicate the LOD.
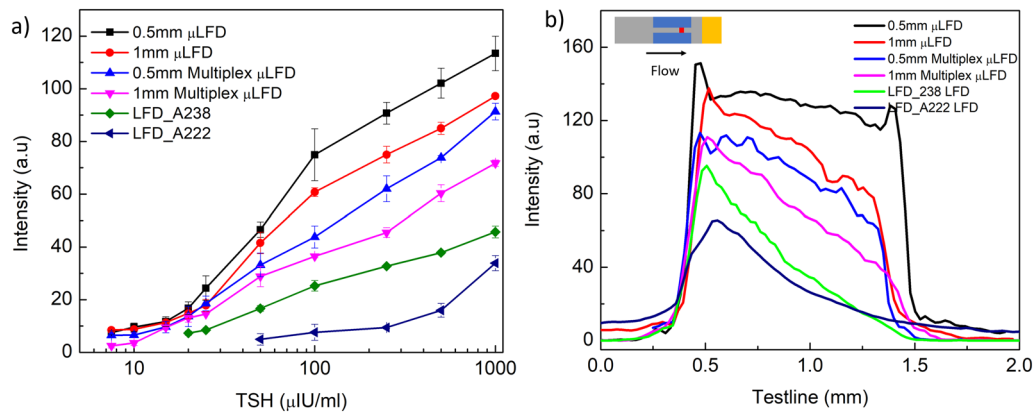
FIG. 4. (a) Average test line intensities at various concentrations of the TSH on all LFDs and (b) test line intensity profiles on all devices at 1000 μIU/ml concentration of the TSH.

with traditional LFDs. The multiplex format of the μLFD is more suitable for detection of multiple biomarkers on one single strip with increased sensitivity when compared with traditional LFDs. A detailed comparison of the test line intensities on various formats of LFDs is shown in Fig. 4(a).

In the case of traditional LFDs, the test line intensities were not uniformly distributed, i.e., higher intensities were present at the beginning of the test line, and weaker intensities were present at the end of the test line, while uniform binding of AuNPs over the test line was formed for μLFDs due to the narrow flow paths, as shown in Fig. 4(b). It can be observed that binding of the AuNPs is more uniform in the case of 0.5 mm μLFDs. Thus, leading edge binding is minimized in the case of μLFDs, which can result in an accurate quantitative analysis of biomarkers by using lateral flow assay readers.

In the case of multiplex μLFDs, absorbent pads (A222 and A238) have not shown any difference on the brightness of the test line, as shown in Fig. 5(a). In addition, for multiplex μLFDs, the brightness of the test lines was the same when measured in serum samples, as shown in Fig. S1. This indicates that in the case of μLFDs, only patterning significantly lowers the flow rate so that the effect of the absorbent pad or viscosity of the samples is nullified. To investigate the effect of constriction width on the multiplex devices, μLFDs were fabricated with four channels where the width of alternating channels is 1 mm and 0.5 mm, as shown in Fig. S2. It has been observed that the brightness of the test line is the same on both 1 mm and 0.5 mm channels, as shown Fig. S3. In addition, the brightness of the test line is the same as in the case of the device consisting of three channels of 1 mm width. This indicates that the brightness of the test line depends on the total width of the channels but not on the width of the single channel in the device.

For all the formats of LFDs, the wicking time for 60 μl of the sample solution is shown in Fig. 5(b). It can be observed from Fig. 5(b) that the 0.5 mm channel provides a slow flow rate and the LFD consisting of the absorbent pad A222 provides a faster flow rate. Accordingly, a decrease in the LOD, an increase in sensitivity, and uniform binding of AuNPs were observed on the LFD providing a slower fluid flow rate and consisting of a smaller test zone.
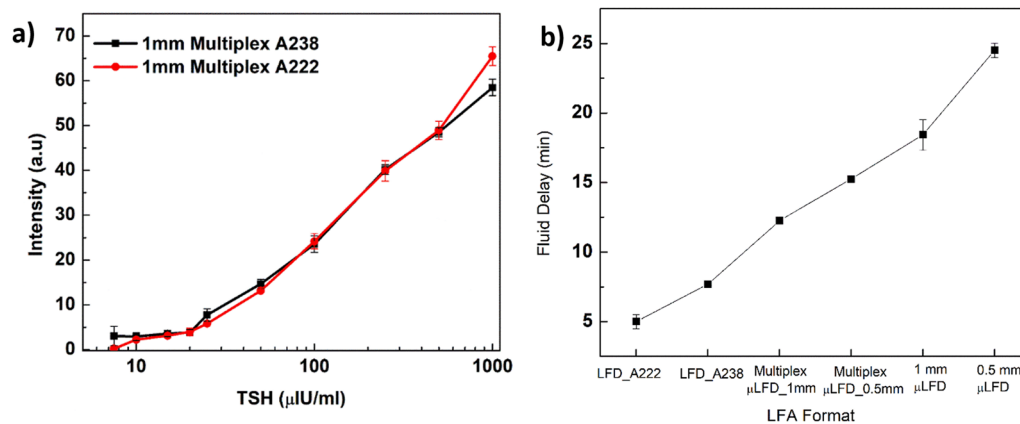

FIG. 5. (a) Shows the brightness of the test line on 1 mm multiplex devices attached to A222 and A238 absorbent pads and (b) the assay time or wicking time for 60 μl of the sample on various formats of LFDs.

IV. CONCLUSIONS

We have presented a novel strategy for improving sensitivity and LOD by patterning the NC membrane with a CO_2 laser to constrain fluid flow. These paper microchannels decrease the test area zone and fluid flow rate, thereby increasing reaction time between the antigen and the capture antibody, leading to the effective formation of the immunocomplex over the test region. Different designs were studied, and paper microchannels of 0.5 mm width exhibited improvement in sensitivity by nine times and LOD by 6.6 times when compared with the traditional LFD. The enhancement in width LOD up to 7.5 μIU/ml can make μLFDs suitable for detection of TSH levels in the clinical domain. This approach of creating narrow constrictions is simpler, is less time consuming, does not require any additional materials to create hydrophobic barriers, and does not need any alterations to the configuration of the LFD when compared with wax printed devices. The proposed method can extend the scope of the LFD with patterned techniques to enable its use in a broad range of applications. This study has shown some very promising data and considerations that are worthy of further research to determine its suitability for a commercial diagnostic test. Further research will be carried out toward multiplex detection of biomarkers including control lines by using serum samples with a complete device geometry.

SUPPLEMENTARY MATERIAL

See the supplementary material for experimental data related to serum and constriction width experiments.

AUTHORS' CONTRIBUTIONS

S.K.B., S.E.M., and E.L.M. designed and performed all the experiments and wrote the paper. J.M., S.M., P.V., and H.M. managed the project and reviewed the manuscript.

ACKNOWLEDGMENTS

DATA AVAILABILITY

The data that support the findings of this study are available from the corresponding author upon reasonable request.

REFERENCES

[1] E. M. Linares, L. T. Kubota, J. Michaelis, and S. Thalhammer, J. Immunol. Methods **375**, 264 (2012).

[2] M. Rayev and K. Shmagel, J. Immunol. Methods **336**, 9 (2008).

[3] X. Hu, J. Liu, Y. Zhang, J. Lu, and L. Zeng, Biosci., Biotechnol., Biochem. **81**, 1874 (2017).

[4] L. Yu, P. Li, X. Ding, and Q. Zhang, Talanta **165**, 167 (2017).

[5] S. K. Vashist, E. Marion Schneider, R. Zengerle, F. von Stetten, and J. H. T. Luong, Biosens. Bioelectron. **66**, 169 (2015).

[6] E. Juntunen, T. Myyryläinen, T. Salminen, T. Soukka, and K. Pettersson, Anal. Biochem. **428**, 31 (2012).

[7] Y. Wang, C. Fill, and S. R. Nugen, Biosensors **2**, 32 (2012).

[8] S. Ramachandran, E. Fu, B. Lutz, and P. Yager, Analyst **139**, 1456 (2014).

[9] S. Kumar, P. Bhushan, V. Krishna, and S. Bhattacharya, Biomicrofluidics **12**, 034104 (2018).

[10] C.-W. Yen, H. de Puig, J. O. Tam, J. Gómez-Márquez, I. Bosch, K. Hamad-Schifferli, and L. Gehrke, Lab Chip **15**, 1638 (2015).

[11] C. N. Loynachan, M. R. Thomas, E. R. Gray, D. A. Richards, J. Kim, B. S. Miller, J. C. Brookes, S. Agarwal, V. Chudasama, R. A. McKendry, and M. M. Stevens, ACS Nano **12**, 279 (2018).

[12] Z. Gao, H. Ye, D. Tang, J. Tao, S. Habibi, A. Minerick, D. Tang, and X. Xia, Nano Lett. **17**, 5572 (2017).

[13] H. Ye and X. Xia, J. Mater. Chem. B **6**, 7102 (2018).

[14] M. Boyd-Moss, S. Baratchi, M. Di Venere, and K. Khoshmanesh, Lab Chip **16**, 3177 (2016).

[15] C. D. Chin, V. Linder, and S. K. Sia, Lab Chip **7**, 41 (2007).

[16] M. Santhiago, E. W. Nery, G. P. Santos, and L. T. Kubota, Bioanalysis **6**, 89 (2014).

[17] Y. Zhang, J. Bai, and J. Y. Ying, Lab Chip **15**, 1465 (2015).

[18] J. Wang, H. Ahmad, C. Ma, Q. Shi, O. Vermesh, U. Vermesh, and J. Heath, Lab Chip **10**, 3157 (2010).

[19] L. Rivas, M. Medina-Sánchez, A. de la Escosura-Muñiz, and A. Merkoçi, Lab Chip **14**, 4406 (2014).

[20] J. R. Choi, Z. Liu, J. Hu, R. Tang, Y. Gong, S. Feng, H. Ren, T. Wen, H. Yang, Z. Qu, B. Pingguan-Murphy, and F. Xu, Anal. Chem. **88**, 6254 (2016).

[21] R. H. Tang, H. Yang, J. R. Choi, Y. Gong, S. S. Feng, B. Pingguan-Murphy, Q. S. Huang, J. L. Shi, Q. B. Mei, and F. Xu, Crit. Rev. Biotechnol. **37**, 411 (2017).

[22] J. R. Choi, K. W. Yong, R. Tang, Y. Gong, T. Wen, H. Yang, A. Li, Y. C. Chia, B. Pingguan-Murphy, and F. Xu, Adv. Healthcare Mater. **6**, 1600920 (2017).

[23] I. N. Katis, P. J. W. He, R. W. Eason, and C. L. Sones, Biosens. Bioelectron. **113**, 95 (2018).

[24] P. J. W. He, I. N. Katis, R. W. Eason, and C. L. Sones, Biomicrofluidics **9**, 026503 (2015).

[25] C. Parolo, M. Medina-Sánchez, A. de la Escosura-Muñiz, and A. Merkoçi, Lab Chip **13**, 386 (2013).

[26] A. Zadehkafi, M. Siavashi, S. Asiaei, and M. R. Bidgoli, J. Chromatogr. B **1110-1111**, 1 (2019).

[27] J. Nie, Y. Liang, Y. Zhang, S. Le, D. Li, and S. Zhang, Analyst **138**, 671 (2013).

[28] X. Song, S. R. Feaster, J. M. Takeuchi, and K. Yang, U.S. patent 2010/0159599 A1 (24 June 2010).

[29] M. A. Mahmud, E. J. M. Blondeel, and B. D. MacDonald, Biomicrofluidics **14**, 014107 (2020).

[30] M. A. Mahmud, E. J. M. Blondeel, M. Kaddoura, and B. D. MacDonald, Micromachines **9**, 220 (2018).

[31] N. Kochupillai and M. Mehta, Rev. Endocr. Metab. Disord. **9**, 237 (2008).

[32] T. S. Scanlan, K. L. Suchland, M. E. Hart, G. Chiellini, Y. Huang, P. J. Kruzich, S. Frascarelli, D. A. Crossley II, J. R. Bunzow, S. Ronca-Testoni, E. T. Lin, D. Hatton, R. Zucchi, and D. K. Grandy, Nat. Med. **10**, 638 (2004).

[33] R. V. Weatherman, ACS Chem. Biol. **2**, 377 (2007).

[34] M. Moreno, P. de Lange, A. Lombardi, E. Silvestri, A. Lanni, and F. Goglia, Thyroid **18**, 239 (2008).

[35] Y. Liu, Q. Zhang, H. Wang, Y. Yuan, Y. Chai, and R. Yuan, Biosens. Bioelectron. **71**, 164 (2015).

[36] S. Choi, J. Hwang, S. Lee, D. W. Lim, H. Joo, and J. Choo, Sens. Actuators, B **240**, 358 (2017).

[37] D. J. You, T. S. Park, and J.-Y. Yoon, Biosens. Bioelectron. **40**, 180 (2013).

[38] E. C. Ridgway and M. T. McDermott, J. Clin. Endocrinol. Metab. **86**, 4585 (2001).

[39] H. Beitollahi, S. G. Ivari, and M. Torkzadeh-Mahani, Biosens. Bioelectron. **110**, 97 (2018).

[40] J. P. He, N. I. Katis, W. R. Eason, and L. C. Sones, Biosensors **8**, 97 (2018).

[41] M. V. Humbert, L. E. Costa, I. Katis, F. Fonseca Ramos, A. Sanchéz Machado, C. Sones, E. A. Ferraz Coelho, and M. Christodoulides, Emerging Microbes Infect. **8**, 1178 (2019).

[42]See http://www.webcitation.org/76RrP6Swk for information on conjugation of antibodies to carboxyl coated gold nanoparticles by using EDC chemistry; accessed 27 March 2019.

[43]M. H. Jazayeri, H. Amani, A. A. Pourfatollah, H. Pazoki-Toroudi, and B. Sedighimoghaddam, Sens. Bio-Sens. Res. **9**, 17 (2016).

[44]J. O. Tam, H. de Puig, C.-w. Yen, I. Bosch, J. Gómez-Márquez, C. Clavet, K. Hamad-Schifferli, and L. Gehrke, J. Immunoassay Immunochem. **38**, 355 (2017).

[45]A. Badu-Tawiah, S. Lathwal, K. Kaastrup, M. Al-Sayah, D. C. Christodouleas, B. S. Smith, G. M. Whitesides, and H. D. Sikes, Lab Chip **15**, 655 (2015).